

# Hyperpolarized $^1\text{H}$ long lived states originating from parahydrogen accessed by rf irradiation<sup>†</sup>

M. B. Franzoni,<sup>\*a</sup> D. Graafen,<sup>a,b</sup> L. Buljubasich,<sup>c</sup> L. M. Schreiber,<sup>b</sup> H. W. Spiess,<sup>a</sup> and K. Münnemann<sup>\*a</sup>

Received Xth XXXXXXXXXXXX 20XX, Accepted Xth XXXXXXXXXXXX 20XX

First published on the web Xth XXXXXXXXXXXX 200X

DOI: 10.1039/b000000x

Hyperpolarization has found many applications in Nuclear Magnetic Resonance (NMR) and Magnetic Resonance Imaging (MRI). However, its usage is still limited to the observation of relatively fast processes because of its short lifetimes. This issue can be circumvented by storing the hyperpolarization in a slowly relaxing singlet state. Symmetrical molecules hyperpolarized by Parahydrogen Induced Hyperpolarization (PHIP) provide a straightforward access to hyperpolarized singlet states because the initial parahydrogen singlet state is preserved at almost any magnetic field strength. In these systems, which show a remarkably long  $^1\text{H}$  singlet state lifetime of several minutes, the conversion of the NMR silent singlet state to observable magnetization is feasible due to the existence of singlet-triplet level anti-crossings. Here, we demonstrate that scaling the chemical shift Hamiltonian by rf irradiation is sufficient to transform the singlet into an observable triplet state. Moreover, because the application of one long rf pulse is only partially converting the singlet state, we developed a multiconversion sequence consisting of a train of long rf pulses resulting in successive singlet to triplet conversions. This sequence is used to measure the singlet state relaxation time in a simple way at two different magnetic fields. We show that this approach is valid for almost any magnetic field strength and can be performed even in the less homogeneous field of an MRI scanner, allowing for new applications of hyperpolarized NMR and MRI.

## 1 Introduction

Nuclear Magnetic Resonance (NMR) is a very important analytical technique widely used in chemistry, physics, medicine and biology. Despite its widespread use, the application of NMR is sometimes hindered because of its low sensitivity: due to the small Zeeman splitting of the energy levels compared with the thermal energy at room temperature, the polarization of a sample is very small even at high magnetic fields<sup>1,2</sup>. Hyperpolarization techniques such as DNP<sup>1,3</sup>, CIDNP<sup>4-6</sup> laser polarized noble gases<sup>7-9</sup> and the here used parahydrogen Induced Polarization (PHIP)<sup>10-12</sup> method have been introduced to overcome this limitation. PHIP employs a hydrogenation reaction with parahydrogen ( $\text{pH}_2$ ) enriched gas, that adds the two hydrogen atoms of a  $\text{pH}_2$  molecule pairwise into a target molecule. Parahydrogen is the nuclear spin singlet state isomer of the  $\text{H}_2$  molecule and the relative orientation

of its nuclear spins (antisymmetric with respect to spin permutations) is conserved after the reaction. As a result of this non-equilibrium state, the observed NMR signal is dramatically increased<sup>13,14</sup>.

However, the hyperpolarization approach is restricted to relatively short time scales (depending on the spin-lattice relaxation time  $T_1$  of the hyperpolarized nuclei, typically on the order of several seconds to at best a few minutes). This lifetime issue limits the application of hyperpolarization to the observation of sufficiently fast processes, e.g. fast chemical reactions<sup>15,16</sup> or metabolism pathways<sup>17-19</sup>. Thus, during the last few years, a lot of research was conducted to overcome this issue. One possibility is to reduce the number of relaxation partners of the hyperpolarized nuclei by simply deuterating the molecule<sup>19</sup>. Another and even more promising approach is the storage of the hyperpolarization in a slowly relaxing singlet state which can be formed by two strongly coupled spins  $\frac{1}{2}$ <sup>20,21</sup>. For this purpose, typically an rf pulse sequence is applied to convert transverse magnetization into singlet state order. Levitt and coworkers<sup>22,23</sup> have developed the known M2S (magnetization to singlet) pulse sequence, which consists of two trains of  $\pi$  pulses. The temporal window between pulses is carefully synchronized with the evolutions due to scalar coupling and chemical shifts of the particular pair.

<sup>†</sup> Electronic Supplementary Information (ESI) available: [details of any supplementary information available should be included here]. See DOI: 10.1039/b000000x/

<sup>a</sup> Max Planck Institute for Polymer Research, Ackermannweg 10, 55128 Mainz, Germany

<sup>b</sup> Johannes Gutenberg University Medical Center, Section of Medical Physics, Mainz, Germany

<sup>c</sup> FAMAFA Universidad Nacional de Córdoba, IFEG CONICET, X5016LAE Córdoba, Argentina

Using PHIP, it has been shown that the original singlet state of parahydrogen can be preserved in a target molecule at low fields<sup>24,25</sup> or even at high fields<sup>26</sup>, resulting in an extension of the relaxation time up to one order of magnitude. At low fields, the two former p<sub>H</sub><sub>2</sub> spins remain strongly coupled in the target molecule and, consequently, the singlet state remains an eigenstate which is naturally preserved. At high field, this is in general more complicated since the chemical shift difference of the two spins prevents the singlet state from being an eigenstate. In our previous work we showed that this problem can be overcome by using a Symmetrical molecule where the p<sub>H</sub><sub>2</sub> atoms remain chemically equivalent and thus strongly coupled at every magnetic field strength<sup>26,27</sup>. The symmetrical molecules allow for long storage of the p<sub>H</sub><sub>2</sub> singlet state. However, the singlet state (total spin 0) is not observable by NMR and must be converted into a triplet state to achieve observable magnetization. For dimethyl maleate, a symmetrical molecule, an anti-crossing of singlet and triplet levels at a particular magnetic field, in the following we call this the resonance field, was identified which allows for the transition to occur<sup>27</sup>. Moving the sample to that resonance field thus leads to observation of the NMR signal of the triplet state. In the present work, we show that it is possible to conveniently generate the singlet-triplet transition inside the observation field of an MRI scanner or NMR spectrometer without moving the sample by applying an off-resonance long rf pulse (also known as Continuous Wave (CW) for historical reasons). With this approach we are able to eliminate the need to physically move the sample which would be a problem for in vivo applications. To demonstrate the versatility of the proposed method, the experiments are performed in a clinical 1.5 T magnetic resonance imaging (MRI) system and in a 7 T magnet for NMR spectroscopy.

Additionally, the efficiency of the sequence is tested experimentally and the very advantageous possibility to generate multiple singlet-triplet conversions within the same train of acquisitions is shown. With the multiconversion methodology, the relaxation lifetime of the singlet state  $T_s$  in the two mentioned magnetic fields is measured and the results are compared.

## 2 Energy level anti-crossings allow singlet-triplet transition

In our previous publications<sup>26,27</sup> we have shown that even though the original singlet state of the p<sub>H</sub><sub>2</sub> molecule is preserved in a symmetrical molecule it is possible to use it as a source of observable hyperpolarization by inducing a singlet-triplet transition. A thorough study<sup>27</sup> demonstrated that this is possible because of the existence of energy level anti-crossings. In the next subsection we will briefly review how the singlet-

triplet transition generating high observable polarization can be simply achieved by moving the sample to a dedicated external magnetic field  $B_0$ .

### 2.1 Field cycling: changing $B_0$

When acetylenedicarboxylic acid dimethyl ester is hydrogenated with parahydrogen to generate maleic acid dimethyl ester, the atoms of the p<sub>H</sub><sub>2</sub> molecule occupy chemically equivalent vinylene (V) positions in the symmetrical molecule<sup>28</sup>, see Fig. 1. For this reason, both spins remain strongly coupled for every magnetic field strength. A 4-spin system is used to model the relevant coupling network of maleic acid dimethyl ester (Fig. 1). The model considers two pairs of chemically equivalent spins. The first pair comprises the two former p<sub>H</sub><sub>2</sub> atoms (the vinylene protons are denoted as V and V'). The second pair is formed by the two methyl groups that can be simplified as single spin 1/2 due to their fast rotation and are denoted as M and M'.

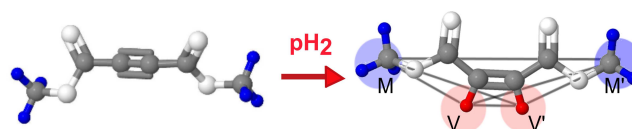


**Fig. 1** Hydrogenation with p<sub>H</sub><sub>2</sub> of acetylenedicarboxylic acid dimethyl ester generates maleic acid dimethyl ester. After hydrogenation the former p<sub>H</sub><sub>2</sub> protons are at the vinylene group positions, V and V'. On the right side, the product molecule is superimposed by the 4-spin model with each methyl group simplified as singlet spin  $\frac{1}{2}$ , M and M'.

This particular class of a 4-spin system is normally denoted as an AA'XX' system and the Hamiltonian in the laboratory frame is written as:

$$\mathcal{H}^{Lab} = \mathcal{H}_z^{Lab} + \mathcal{H}_J \quad (1)$$

with the isotropic part of the chemical shift Hamiltonian being:

$$\mathcal{H}_z^{Lab} = 2\pi\nu_V(I_V^z + I_{V'}^z) + 2\pi\nu_M(I_M^z + I_{M'}^z). \quad (2)$$

The parameter  $\nu_V$  corresponds to the chemically equivalent protons in the vinylene group and  $\nu_M$  represents the chemical shift of the chemically equivalent methyl groups, the J-coupling Hamiltonian is given by:

$$\begin{aligned} \mathcal{H}_J = & 2\pi (J_{V,V'} \mathbf{I}_V \cdot \mathbf{I}_{V'} + J_{M,M'} \mathbf{I}_M \cdot \mathbf{I}_{M'}) \\ & + 2\pi J_{V,M} (\mathbf{I}_V \cdot \mathbf{I}_M + \mathbf{I}_{V'} \cdot \mathbf{I}_{M'}) \\ & + 2\pi J_{V',M} (\mathbf{I}_{V'} \cdot \mathbf{I}_M + \mathbf{I}_V \cdot \mathbf{I}_{M'}). \end{aligned} \quad (3)$$

By choosing a suitable basis constructed as the direct product of the eigenstates of the two strongly coupled former parahydrogen protons (V and V') and the eigenstates of the methyl

groups (M and M'), the eigenvalue problem of equation (1) is solved<sup>27</sup>. Essentially, the problem is reduced to solving the eigenvalue problem of the  $2 \times 2$  matrix ( $\tilde{\mathcal{H}}^{Lab}$ ):

$$\tilde{\mathcal{H}}^{Lab} = \frac{\pi}{2} \begin{pmatrix} J_{V,V'} - 3J_{M,M'} + 4\nu_V & \sqrt{2}(J_{V,M} - J_{V,M'}) \\ \sqrt{2}(J_{V,M} - J_{V,M'}) & J_{M,M'} - 3J_{V,V'} - 4\nu_M \end{pmatrix} \quad (4)$$

By solving the corresponding eigenvalue equation the presence of a level anti-crossing between the eigenstates  $|T_{+1}^{V,V'} S^{M,M'}\rangle$  and  $|S^{V,V'} T_{+1}^{M,M'}\rangle$  (as defined in Eq. (5) in ref<sup>27</sup>) at an exact defined value of the external magnetic field is identified. The magnetic field at the resonance condition that gives rise to the anti-crossing,  $B_R$ , is such that:

$$(\nu_V - \nu_M)|_{B_R} \approx J_{V,V'} \quad (5)$$

The preceding approximation is valid since the coupling  $J_{V,V'}$  is, at least, one order of magnitude larger than the other couplings in the molecule. The condition (5) results for maleic acid dimethyl ester in  $B_R = 0.1$  T.

In Fig. 2a the corresponding energy levels are plotted as a function of the external magnetic field  $B_0$ . From the plot it is clear that the simple physical movement of the sample to the resonance magnetic field  $B_R$  allows the singlet-triplet conversion and consequently the observation of the pH<sub>2</sub> enhanced singlet state. This method was experimentally verified, in particular the marked field dependence of singlet to triplet conversion, and the lifetime of the singlet state ( $T_S = 4$  min) was obtained<sup>26,27</sup>.

## 2.2 Chemical shift scaling: changing $B_1$

The use of long rf pulses to scale the Hamiltonian inside the magnet is a common strategy in traditional NMR<sup>1,2</sup>. It is also not new in singlet state NMR<sup>29–32</sup>, where it is used, e.g., to preserve the singlet state: a long rf pulse with sufficient intensity applied between the resonance frequencies of two inequivalent spins suppresses the difference in chemical shift among the pair. Thus, the nuclear spins become effectively chemically equivalent, which is a requirement to isolate the singlet from the triplet states. This is not necessary in our experiments because, as explained above, chemical equivalence naturally occurs in symmetrical molecules, for every magnetic field strength.

Here, the long rf pulse is used to scale the chemical shift part of the relevant Hamiltonian to access the level anti-crossing region in order to convert the singlet to a triplet state.

For that purpose, it is useful to rewrite the Hamiltonian of the AA'XX' system of equation (2) now in the rotating frame as<sup>30</sup>:

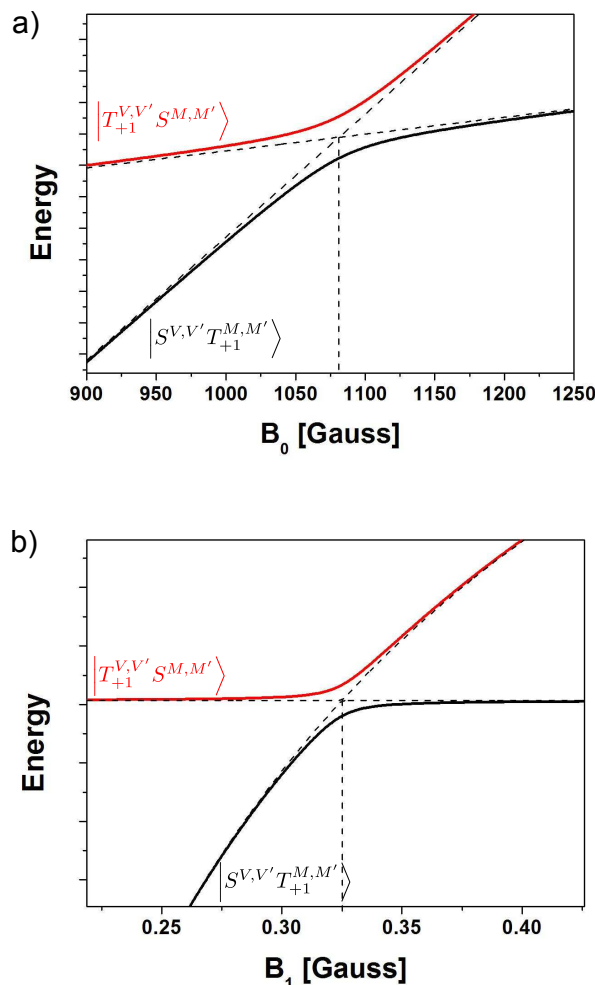


**Fig. 2** Energy level anti-crossing allows the singlet-triplet transition necessary to observe the pH<sub>2</sub> singlet state, at a well defined resonance position. The resonance condition can be reached either by a) field cycling experiment, i.e. changing the  $B_0$  field. b) scaling the chemical shift interaction by applying an rf  $B_1$  field.

$$\mathcal{H}_z = 2\pi\Omega_\Sigma [(I_V^z + I_{V'}^z) + (I_M^z + I_{M'}^z)] + 2\pi\Omega_\Delta [(I_V^z + I_{V'}^z) - (I_M^z + I_{M'}^z)] \quad (6)$$

where  $\Omega_\Sigma = \nu_{rf} - \frac{1}{2}(\nu_V + \nu_M)$  is the offset of the carrier  $\nu_{rf}$  and  $\Omega_\Delta = -\frac{1}{2}(\nu_V - \nu_M)$ .

If the system is irradiated by a continuous rf field, the Hamiltonian governing the system can now be written as:

$$\mathcal{H} = \mathcal{H}_{rf} + \mathcal{H}_z + \mathcal{H}_J \quad (7)$$

with

$$\mathcal{H}_{rf} = 2\pi\nu_1(I_V^x + I_V^x + I_M^x + I_{M'}^x) \quad (8)$$

where  $\nu_1$  corresponds to the  $B_1$  rf amplitude and  $\mathcal{H}_z$  and  $\mathcal{H}_J$  are defined as (6) and (3), respectively. The rf field is assumed to be in  $x$  direction for simplicity, without loss of generality.

In the following calculations, the J-coupling Hamiltonian is not included, since it is composed of scalar contributions which are not affected when rotating the reference frame. Starting with the Zeeman and rf terms of the Hamiltonian:

$$\begin{aligned} \mathcal{H} = & 2\pi\nu_1(I_V^x + I_V^x + I_M^x + I_{M'}^x) \\ & + 2\pi\Omega_\Sigma[(I_V^z + I_{V'}^z) + (I_M^z + I_{M'}^z)] \\ & + 2\pi\Omega_\Delta[(I_V^z + I_{V'}^z) - (I_M^z + I_{M'}^z)], \end{aligned} \quad (9)$$

it is possible to perform a frame transformation to a more convenient set of coordinates  $(\hat{x}', \hat{y}', \hat{z}')$  such that the  $\hat{z}'$  axis:

$$\hat{z}' = \sin(\beta)\hat{x} + \cos(\beta)\hat{z} \quad (10)$$

is aligned with an effective field, with direction  $(\beta)$  and intensities  $(\nu_{eff})$  defined by:

$$\tan(\beta) = \frac{\nu_1}{\Omega_\Sigma} \quad (11)$$

$$\nu_{eff} = \sqrt{\nu_1^2 + \Omega_\Sigma^2}. \quad (12)$$

The Hamiltonian is written in the new reference frame, omitting the primes in the notation, as:

$$\begin{aligned} \mathcal{H} = & 2\pi\nu_{eff}(I_V^z + I_{V'}^z + I_M^z + I_{M'}^z) \\ & + 2\pi\cos(\beta)\Omega_\Delta[(I_V^z + I_{V'}^z) - (I_M^z + I_{M'}^z)] \\ & + 2\pi\sin(\beta)\Omega_\Delta[(I_V^x + I_{V'}^x) - (I_M^x + I_{M'}^x)]. \end{aligned} \quad (13)$$

If  $\frac{\Omega_\Sigma}{\nu_{eff}} \ll 1$ , the last term at the right side of equation (13) (a non-secular term) is negligible for the dynamics. Under this condition, it is straightforward to rewrite equation (13) in the following way:

$$\begin{aligned} \mathcal{H} = & 2\pi\tilde{\nu}_V(I_V^z + I_{V'}^z) \\ & + 2\pi\tilde{\nu}_M(I_M^z + I_{M'}^z), \end{aligned} \quad (14)$$

with  $\tilde{\nu}_V = \nu_{eff} + \cos(\beta)\Omega_\Delta$  and  $\tilde{\nu}_M = \nu_{eff} - \cos(\beta)\Omega_\Delta$ .

It results clear that the dependence on the spin operators of equation (14) is the same as for equation (2). The same procedure applied before works for the Hamiltonian (14). The same basis is chosen and the problem reduces to solving the eigenvalue problem of the  $2 \times 2$  matrix  $\tilde{\mathcal{H}}$ :

$$\tilde{\mathcal{H}} = \frac{\pi}{2} \begin{pmatrix} J_{V,V'} - 3J_{M,M'} + 4\tilde{\nu}_V & \sqrt{2}(J_{V,M} - J_{V,M'}) \\ \sqrt{2}(J_{V,M} - J_{V,M'}) & J_{M,M'} - 3J_{V,V'} - 4\tilde{\nu}_M \end{pmatrix} \quad (15)$$

Again, an energy level anti-crossing is found and the resonance condition is rescaled as follows:

$$\cos(\beta)|_{\beta_R} (\nu_V - \nu_M)|_{B_0} \approx J_{V,V'}. \quad (16)$$

In the previous equation the scaling of the resonance condition achieved by applying a long rf pulse at a well defined offset and with a well defined power, becomes evident and can be obtained for every observation field  $B_0$  by fulfilling:

$$\cos(\beta_R) = \frac{B_R}{B_0}. \quad (17)$$

In practice, it is useful to rewrite the relationship between the RF pulse strength,  $\nu_1$ , and the RF offset,  $\Omega_\Sigma$ , as:

$$\nu_1 = \tan\left(\arccos\left(\frac{B_R}{B_0}\right)\right)\Omega_\Sigma. \quad (18)$$

The requirement  $\Omega_\Sigma \neq 0$  must be satisfied.

As an illustration, in Fig. 2b the solution of equation (15) is plotted as a function of the applied rf field  $B_1$ , for a fixed offset of the carrier  $\Omega_\Sigma = 100$  Hz and at an observation field  $B_0 = 1.5$  T.

## 3 Experimental results

### 3.1 Conversion sequence

In figure 3a, the designed pulse sequence is shown. The initial  $\frac{\pi}{2}$  pulse is applied to ensure that any possible initial magnetization created during the transportation of the sample to the observation field is suppressed. A waiting period time,  $T_W$ , precedes the singlet-triplet conversion by the long rf and the excitation pulses.

The spectrum shown of PHIP-hyperpolarized maleic acid dimethyl ester in Fig. 3b was obtained after a waiting period of  $T_W = 3$  min, which ensures that the hydrogenation reaction has finished when the conversion sequence starts, thus no new singlet state is generated during the measurements. The spectrum was acquired in the 1.5 T MRI scanner with  $\nu_1 = 1355.27$  Hz,  $\Omega_\Sigma = 100$  Hz fulfilling the condition in equation (18). The spectrum shows the  $180^\circ$  phase difference between the vinylene and the methyl group predicted theoretically and observed experimentally with the field cycling method<sup>27</sup>. The amount of singlet state converted into observable triplet state depends on how the level anti-crossing region is approached<sup>33,34</sup>. The amplitude of the vinylene peak was studied as a function of the long rf pulse power ( $\nu_1$ ) and duration ( $d_{rf}$ ) to optimize the conversion, these results are shown in Supplementary Information. The used values  $\nu_1 = 1355.27$  Hz and  $d_{rf} = 5$  sec resulted from this study.

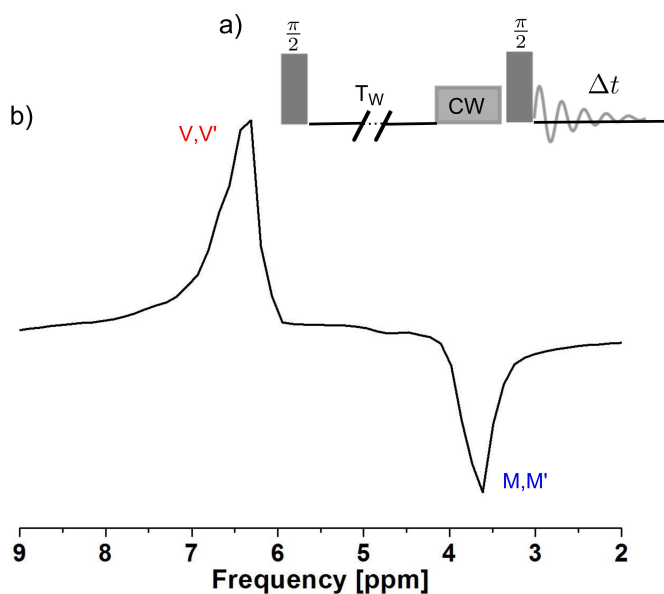


**Fig. 3** a) Pulse sequence for singlet-triplet conversion by applying a long rf pulse. b) Spectrum of PHIP-hyperpolarized maleic acid dimethyl ester obtained after a waiting time  $T_W = 3$  min at 1.5 T. The peaks corresponding to the vinylene and methyl groups are tagged with V,V' and M,M', respectively.

### 3.2 Multiconversion experiments

The application of the long rf pulse is only partially converting the singlet into the triplet state, allowing for the application of a train of long rf pulses with successive singlet to triplet conversions (see Fig. 4a) to achieve multiconversion.

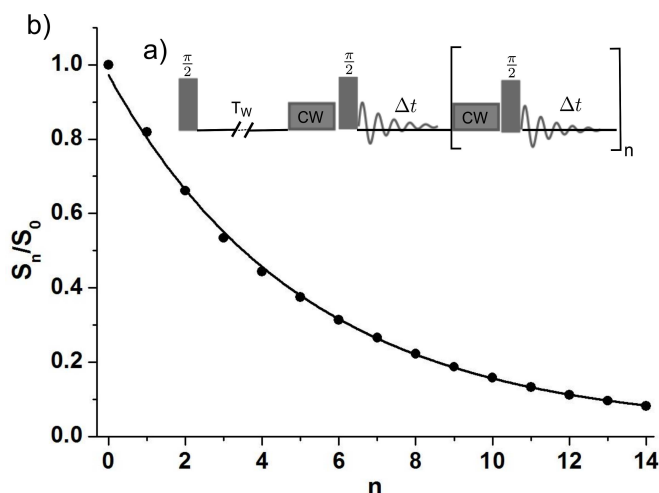


**Fig. 4** a) After the waiting time  $T_W$ , a train of long rf pulses and acquisitions form the multiconversion sequence. b) Integral of the vinylene signal plotted as a function of the number of conversions,  $T_W = 3$  min,  $\Delta t = 25$  s,  $\nu_1 = 1355.8$  Hz and  $d_{rf} = 5$  sec.

In Fig. 4b the decay of the vinylene signal is plotted as a function of the number of conversions ( $n$ ) for a fixed repetition period ( $\Delta t = 25$  sec). The relaxation constant of the singlet state  $T_s$  can not directly be obtained from these experiments, since some external factors as the conversion efficiency and the spin-lattice relaxation unavoidably influence the results.

However, by performing a few experiments with different repetition periods combined with a suitable data processing, it is possible to take into account these intrinsic factors.

The initial signal (after the first conversion) is given by:

$$S_0 = \xi A_S(T_W), \quad (19)$$

with  $A_S(T_W)$  being the amplitude resulting from those molecules in the singlet state after the waiting time  $T_W$ . Strictly, the conversion fraction  $\xi$  is actually  $\xi(\nu_1, d_{rf})$ , as mentioned above, i.e. the effectiveness of the conversion depends on the power ( $\nu_1$ ) and duration ( $d_{rf}$ ) of the long rf pulse.

After the next conversion ( $n=1$ ), the observed signal is

$$\begin{aligned} S_1 &= [A_S(T_W) - \xi A_S(T_W)] \xi \exp\left(-\frac{\Delta t}{T_s}\right) \\ &= S_0(1 - \xi) \exp\left(-\frac{\Delta t}{T_s}\right). \end{aligned} \quad (20)$$

and after  $n$  conversions the signal is:

$$S_n = S_0(1 - \xi)^n \exp\left(-\frac{n\Delta t}{T_s}\right) \quad (21)$$

As can be seen from equation (21) the first signal  $S_0$  can be used for normalization. This is an advantage of the multiconversion method with respect to the field cycling method previously used for the  $T_s$  measurement<sup>26</sup>. With this normalization it is possible to get rid of the influence of the external factors, like the conversion of the hydrogenation reaction or the amount of sample inside the rf coil (experiments using more than one sample are necessary to obtain the characteristic  $T_s$  decay with both methods).

By rearranging the last equation it is possible to write,

$$\frac{S_n}{S_0} = \exp(-D_c(\Delta t)n) \quad (22)$$

with the characteristic decay  $D_c$  defined as,

$$D_c(\Delta t) = \frac{1}{T_s} \Delta t - \ln(1 - \xi). \quad (23)$$

Based on equation (23) we can infer the singlet state relaxation time  $T_s$  and the conversion fraction  $\xi$ . To this end the multiconversion sequence was applied for different repetition periods,  $\Delta t$ . For each  $\Delta t$  the amplitude of the vinylene signal was plotted as a function of the number of conversions and an exponential decay as shown in Fig. 4b, was obtained. Next,

the extracted characteristic decay constants,  $D_c$ , and their deviations were plotted as a function of their corresponding repetition period  $\Delta t$  as shown in figure 5. After a linear fit, the characteristic singlet state relaxation time  $T_s$  and the conversion fraction  $\xi$  were calculated, from the slope and intercept, following expression (23).

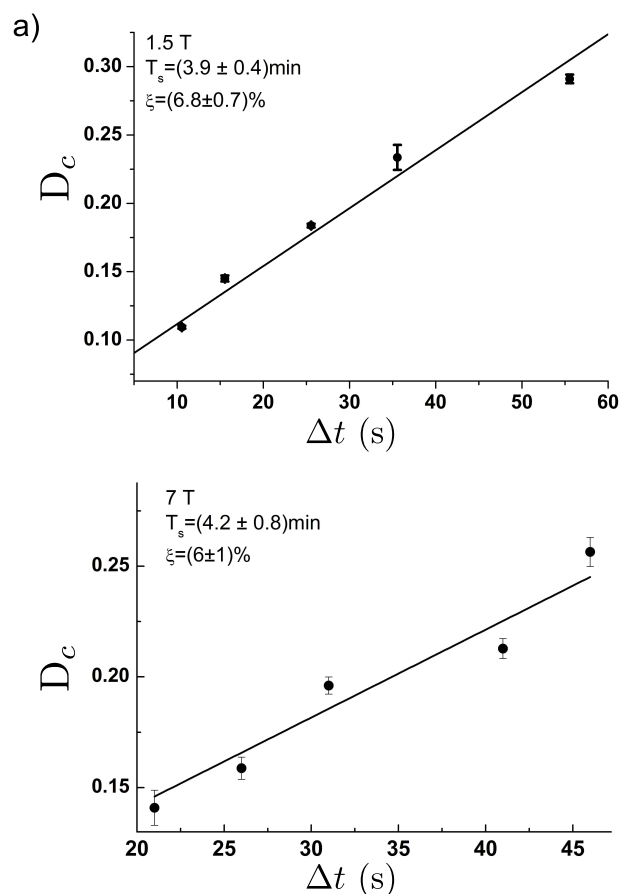


**Fig. 5** Exponential characteristic decay constant  $D_c$  as a function of the repetition time  $\Delta t$  for experiments at a) 1.5 T and b) 7 T. The given error values for each data point are assigned after each exponential fit of the decay curves. The results of the linear fittings are displayed in the respective figures.

Moreover, these experiments were performed in two different magnets: a 1.5 T clinical MRI system and a 7 T NMR spectrometer. The corresponding results are plotted in Fig. 5. For the conversion fraction the values  $\xi = (6.8 \pm 0.7) \%$  at 1.5 T and  $\xi = (6 \pm 1) \%$  at 7 T were obtained. For the singlet state relaxation, the characteristic times resulted in  $T_s = (3.9 \pm 0.4) \text{ min}$  for the 1.5 T magnet and  $T_s = (4.2 \pm 0.8) \text{ min}$  for the 7 T magnet. Both values agree, within the margin of error, with the  $T_s = 4 \text{ min}$  obtained before with the field cycling method

in the 7 T magnet<sup>26</sup>.

As the duration of the long rf pulse (5 seconds) is comparable to the characteristic relaxation times of the triplet state ( $T_1 \approx 10 \text{ sec}$  and  $T_2^*$  some milliseconds) the amplitude of the observed signal after the conversion is also influenced by these relaxation mechanisms. However, because of the used normalization method, these quantities will not affect the values obtained for  $T_s$  and  $\xi$  after the linear fitting.

## 4 Sample and instrumentation

The samples used for the experiments consist of a mixture of 500 mg dimethyl acetylenedicarboxylate (99%, Sigma Aldrich) and 10 mg (0.23 mol%) of the hydrogenation catalyst [1,4-bis(diphenylphosphino) butane] (1,5-cyclo-octadiene) rhodium (I) tetrafluoroborate, dissolved in 2.6 g of acetone- $d_6$  (99.9%  $D$ , Sigma Aldrich). They were prepared in argon atmosphere and filled into 10 mm NMR pressure tubes sealed with a septum cap.  $p\text{H}_2$  enriched to 93% was prepared with a Bruker  $p\text{H}_2$  generator and stored in aluminum cylinders.

At earth magnetic field, the sample was heated up to  $70^\circ\text{C}$  and pressurized with 4 bar of parahydrogen. For the experiments performed with the 7T magnet, the sample was shaken at earth field and then transported to the observation field. In the clinical magnet it was possible to shake the sample in the bore of the magnet, i.e. the observation field. In all experiments the used waiting time was  $T_W = 3 \text{ min}$  to ensure that the hydrogenation reaction has finished before starting the conversion sequence.

The clinical scanner is an 1.5 T MRI system, Magnetom Sonata, Siemens and a finger coil was used in the experiments. The 7 Tesla magnet is equipped with a Bruker Avance II console.

## 5 Discussions

The ability to store the initial hyperpolarized state originating from  $p\text{H}_2$  as a singlet state at nearly every magnetic field and to convert it to an observable NMR signal just by applying an r.f. pulse, may open up many new applications for hyperpolarized NMR. We have demonstrated that the method works even in the inhomogeneous magnetic field of an MRI scanner thus it might be very useful for in vivo MRI, using PHIP polarized molecules as contrast agents.

As mentioned above, the application of a long rf pulse is not new in singlet state NMR<sup>29,30,32</sup>, however in this work it is used with a different purpose. In the previous studies, the long rf pulse sequence was applied to force a spin system to a state that is not an eigenstate, and depending on the spin system the requirements for the spin-locking pulse can be very demanding<sup>31</sup>. On the other hand, in this work the initial  $p\text{H}_2$

singlet state is preserved without any pulse application and the long rf pulse is applied only for observation. Therefore relatively short pulses which deposit not too much energy in the sample can be used.

The multiconversion method developed offers the possibility of accessing the characteristic singlet state relaxation time  $T_s$  in a simple way or to subsequently use the singlet state signal for different purposes within the same experiment. The experiments were performed in two different magnets to show not only the generality of the method but also, to get some hints on  $T_s$  relaxation mechanisms. Within the margin of error, the same  $T_s$  values were obtained at 1.5 T and 7 T. It can then be inferred that, as expected for this particular symmetrical molecule, chemical shift anisotropy is not the mechanism producing the observed  $T_s$  relaxation. Further studies are in progress to identify the leading relaxation mechanisms for this kind of symmetrical molecules.

The results introduced here represent a new approach to induce the singlet to triplet conversion other than the dedicated pulse rf sequences proved to work among chemically inequivalent<sup>20,35</sup>; nearly equivalent<sup>23,36</sup> and equivalent<sup>37</sup> spin pairs. For instance, in the last case<sup>37</sup>, Feng et al. have shown for a doubly labeled  $^{13}\text{C}$  molecule the possibility to induce the transition without breaking the molecular symmetry and without moving the sample, using a different approach. In this work they showed that the sequence M2S-S2M, can also be used if the spin pair is chemically equivalent but not magnetically equivalent. One of the requirements of the mentioned sequence is that the temporal intervals between pulses and total number of applied pulses, must satisfy a particular condition function of the couplings of the molecule. To this end, all relevant parameters must be known. On the other hand, the method presented here using the scaling of the chemical shift Hamiltonian, does not strictly require the knowledge of all coupling parameters. As previously demonstrated<sup>27</sup>, the resonance magnetic field can be obtained empirically, e.g., in a field-cycling experiment. Thus, the scaling factor can be obtained without any previous knowledge of the molecule parameters.

The efficiency of the conversion sequence presented in this work (approx 6%) is similar to the one obtained by Feng et al. (approx 5%). These values are not very encouraging when compared to the efficiency reported for example in the case of nearly equivalent spins by Laustsen et al.<sup>36</sup> (50%) or to the theoretical estimation for the M2S sequence (67%). We assume that this difference is based on the fact that when dealing with chemically equivalent spins the singlet state is essentially an eigenstate at every magnetic field and the transition is less probable to occur and thus more difficult to induce. However, as shown in this work, this low conversion can also be an advantage since it allows for multiconversion experiments.

The theoretical understandings of level anti-crossings in-

roduced in our previous work<sup>27</sup> and by Miesel *et al.*<sup>38</sup> together with the here presented results might be also exploited for transferring the singlet state enhanced signal to only one specific nucleus in the molecule at any magnetic field strength.

Finally, we have shown that the necessary lifetime prolongation of hyperpolarization by singlet state storage, can be achieved in a comfortable way using PHIP polarized symmetrical molecules and long rf pulses converting it into an observable signal enhancement.

## 6 Acknowledgements

The authors gratefully acknowledge financial support by the Max Planck Society, the Max Planck Graduate center with Johannes Gutenberg-University Mainz (MPGC) and the Federal Ministry of Education and Research (VIP0327). We are also grateful to Lic. Ignacio Prina for experimental help. and Dr. Konstantin L. Ivanov for stimulating discussions.

## References

- 1 A. Abragam, *Principles of Nuclear Magnetism*, Oxford University Press, USA, 1983.
- 2 C. P. Slichter, *Principles of Magnetic Resonance*, Springer, Softcover reprint of hardcover 3rd ed. 1990 edn., 2010.
- 3 J. H. Ardenkjaer-Larsen, *P. Natl. Acad. Sci.*, 2003, **100**, 10158–10163.
- 4 J. Bargon, H. Fischer and U. Johnsen, *Z. Naturforsch. Pt. A*, 1967, **A 22**, 1551–1555.
- 5 J. Bargon, *Helvetica Chimica Acta*, 2006, **89**, 2082–2102.
- 6 R. Lawler, *J. Am. Chem. Soc.*, 1967, **89**, 5519–5521.
- 7 N. Bhaskar, W. Happer and T. McClelland, *Phys. Rev. Lett.*, 1982, **49**, 25–28.
- 8 T. G. Walker and W. Happer, *Rev. Mod. Phys.*, 1997, **69**, 629–642.
- 9 R. H. Acosta, P. Blümler, K. Münnemann and H.-W. Spiess, *Prog. Nucl. Mag Res. Sp.*, 2012, **66**, 40–69.
- 10 C. R. Bowers and D. P. Weitekamp, *Phys. Rev. Lett.*, 1986, **57**, 2645–2648.
- 11 K. Münnemann and H. W. Spiess, *Nat. Phys.*, 2011, **7**, 522–523.
- 12 R. A. Green, R. W. Adams, S. B. Duckett, R. E. Mewis, D. C. Williamson and G. G. Green, *Prog. Nuc. Mag. Res. Sp.*, 2012, **67**, 1–48.
- 13 D. Canet, C. Aroulanda, P. Mutzenhardt, S. Aime, R. Gobetto and F. Reineri, *Concept. Magn. Reson. A*, 2006, **28A**, 321–330.
- 14 C. R. Bowers, in *Encyclopedia of Magnetic Resonance*, John Wiley & Sons, Ltd, 2007.
- 15 Y. Lee, G. S. Heo, H. Zeng, K. L. Wooley and C. Hilty, *J. Am. Chem. Soc.*, 2013, **135**, 4636–4639.
- 16 M. Duenkel, N. Vogel, C. K. Weiss, K. Landfester, H.-W. Spiess and K. Münnemann, *Macromolecules*, 2012, **45**, 1839–1846.
- 17 K. Golman, R. in't Zandt, M. Lerche, R. Pehrson and J. H. Ardenkjaer-Larsen, *Cancer Res.*, 2006, **66**, 10855–10860.
- 18 D. M. Wilson, K. R. Keshari, P. E. Z. Larson, A. P. Chen, S. Hu, M. Van Criekinge, R. Bok, S. J. Nelson, J. M. Macdonald, D. B. Vigneron and J. Kurhanewicz, *J. Magn. Reson.*, 2010, **205**, 141–147.
- 19 N. M. Zacharias, H. R. Chan, N. Sailasuta, B. D. Ross and P. Bhat-tacharya, *J. Am. Chem. Soc.*, 2012, **134**, 934–943.
- 20 M. Carravetta, O. G. Johannessen and M. H. Levitt, *Phys. Rev. Lett.*, 2004, **92**, 153003.
- 21 M. H. Levitt, *Annu. Rev. Phys. Chem.*, 2012, **63**, 89–105.

- 
- 22 G. Pileio, M. Carravetta and M. H. Levitt, *P. Natl. Acad. Sci.*, 2010, **107**, 17135–17139.
  - 23 M. C. D. Tayler and M. H. Levitt, *Phys. Chem. Chem. Phys.*, 2011, **13**, 5556–5560.
  - 24 D. Canet, S. Bouguet-Bonnet, C. Aroulanda and F. Reineri, *J. Am. Chem. Soc.*, 2007, **129**, 1445–1449.
  - 25 E. Vinogradov and A. K. Grant, *J. Magn. Reson.*, 2008, **194**, 46–57.
  - 26 M. B. Franzoni, L. Buljubasich, H. W. Spiess and K. Münnemann, *J. Am. Chem. Soc.*, 2012, **134**, 10393–10396.
  - 27 L. Buljubasich, M. B. Franzoni, H. W. Spiess and K. Münnemann, *J. Magn. Reson.*, 2012, **219**, 33–40.
  - 28 M. Haake, J. Barkemeyer and J. Bargon, *J. Phys. Chem.*, 1995, **99**, 17539–17543.
  - 29 M. Carravetta and M. H. Levitt, *J. Am. Chem. Soc.*, 2004, **126**, 6228–6229.
  - 30 K. Gopalakrishnan and G. Bodenhausen, *J. Magn. Reson.*, 2006, **182**, 254–259.
  - 31 G. Pileio and M. H. Levitt, *J. Chem. Phys.*, 2009, **130**, 214501–214501–14.
  - 32 S. J. DeVience, R. L. Walsworth and M. S. Rosen, *J. Magn. Reson.*, 2012, **218**, 5–10.
  - 33 L. D. Landau, *Phys. Z. Sow.*, 1932, **2**, 46–51.
  - 34 C. Zener, *Proc. R. Soc. Lond. Ser. A*, 1932, **137**, 696–702.
  - 35 R. Sarkar, P. R. Vasos and G. Bodenhausen, *J. Am. Chem. Soc.*, 2006, **129**, 328–334.
  - 36 C. Laustsen, G. Pileio, M. C. D. Tayler, L. J. Brown, R. C. D. Brown, M. H. Levitt and J. H. Ardenkjaer-Larsen, *Magn. Res. Med.*, 2012, **68**, 1262–1265.
  - 37 Y. Feng, R. M. Davis and W. S. Warren, *Nature Physics*, 2012, **8**, 831–837.
  - 38 K. Miesel, K. Ivanov, A. Yurkovskaya and H.-M. Vieth, *Chem. Phys. Lett.*, 2006, **425**, 71–76.